

## Supporting Information

### Inhibition of Tau Filament Formation by Conformational Modulation

Elias Akoury<sup>a</sup>, Michal Gajda<sup>a</sup>, Marcus Pickhardt<sup>b</sup>, Jacek Biernat<sup>b</sup>, Pornsuwan Soraya<sup>d</sup>, Christian Griesinger<sup>a</sup>, Eckhard Mandelkow<sup>b,c</sup>, and Markus Zweckstetter<sup>a,c</sup>

<sup>a</sup> Department for NMR-based Structural Biology, Max Planck Institute for Biophysical Chemistry, 37077 Göttingen, Germany.

<sup>b</sup> German Center for Neurodegenerative Diseases (DZNE), Ludwig-Erhard-Allee 2, 53175 Bonn, Germany. <sup>c</sup> CAESAR Research Center, Ludwig-Erhard-Allee 2, 53175 Bonn, Germany. <sup>d</sup> RG Electron Spin Resonance Spectroscopy, Max Planck Institute for Biophysical Chemistry, Am Fassberg 11, 37077 Göttingen, Germany. <sup>e</sup> German Center for Neurodegenerative Diseases (DZNE), Göttingen, Germany.

#### SUPPORTING FIGURES

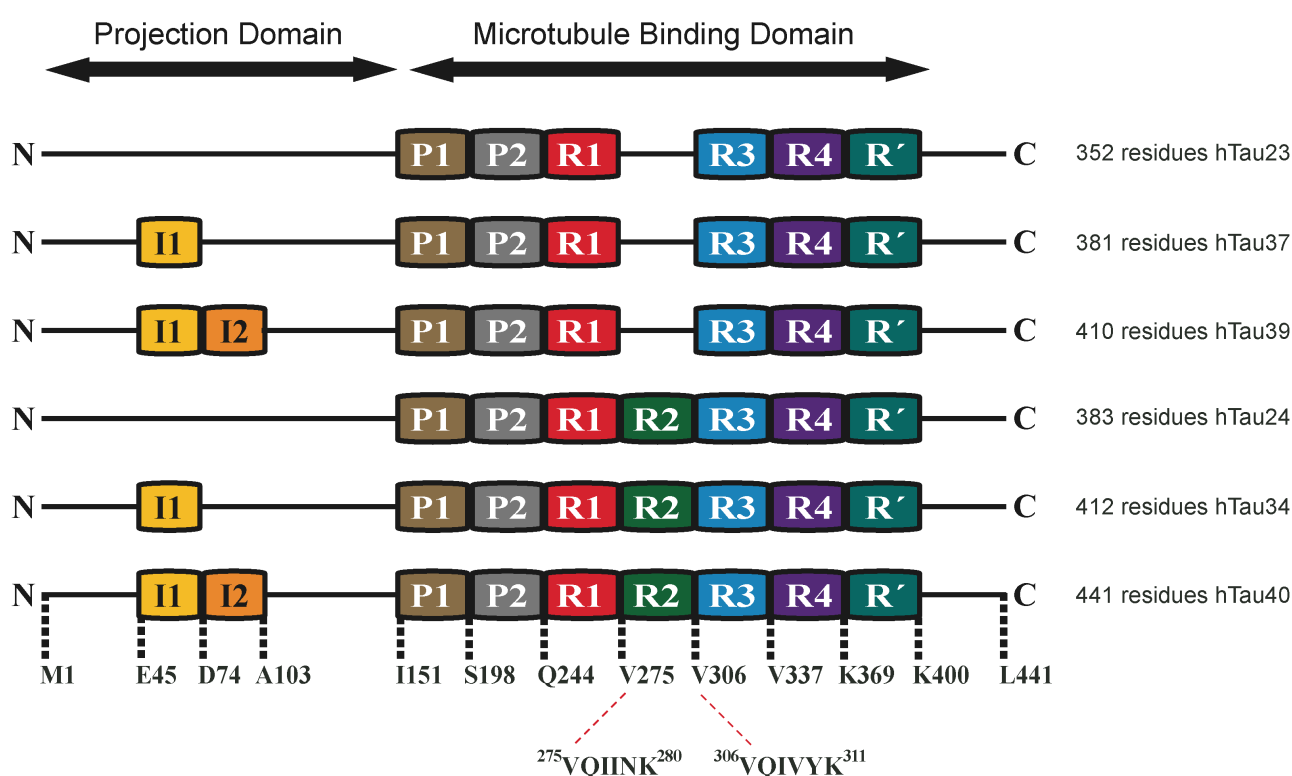


**Figure S1. Isoforms of human Tau protein.** Six isoforms of Tau protein exist in the human central nervous system and are generated by alternative splicing of the MAPT gene. The number of the insert regions in the projection domain (0, 1 or 2) and the presence or absence of the second repeat region in the microtubule-binding domain distinguish them. N or C = N or C-terminus, I = insert, P = proline-rich region, and R = repeat region.

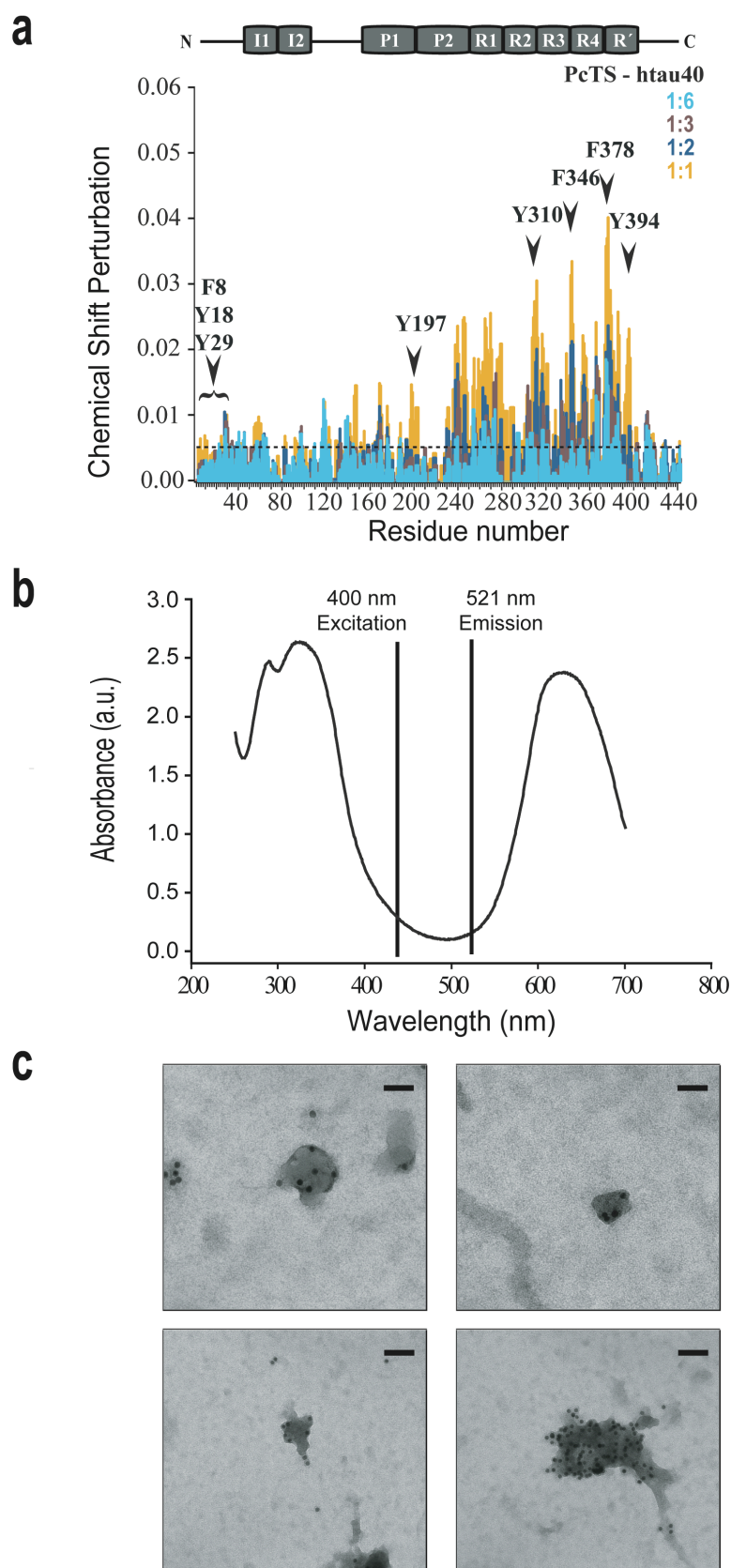


**Figure S2.** (a) Chemical shift deviations ( $\Delta\delta_{1H/15N_{tit}} - \Delta\delta_{1H/15N_{ref}}$ ) observed in 2D  $^1H$ - $^{15}N$  HSQC NMR spectra of htau40wt at increasing PcTS concentrations. Averaged, normalized chemical shift deviations were calculated according to  $\Delta\delta_{AV} = [0.5(\delta_{H_{tit}} - \delta_{H_{wt}})^2 + 0.02(\delta_{N_{tit}} - \delta_{N_{wt}})^2]^{1/2}$ . Dotted black lines correspond to thresholds of chemical shift perturbations of 0.005 ppm for PcTS. (b) Absorption profile of PcTS demonstrating that the absorption properties of PcTS do not interfere with ThS fluorescence in the working range (excitation and emission wavelengths of 440 nm and 521 nm, respectively). (c) Electron micrographs of PcTS-htau40 oligomers. Scale bars, 40 nm (upper panels) and 70 nm (lower panels). The black dots represent the gold-labelled antibody K9JA-gold<sub>10nm</sub> used for immunostaining.

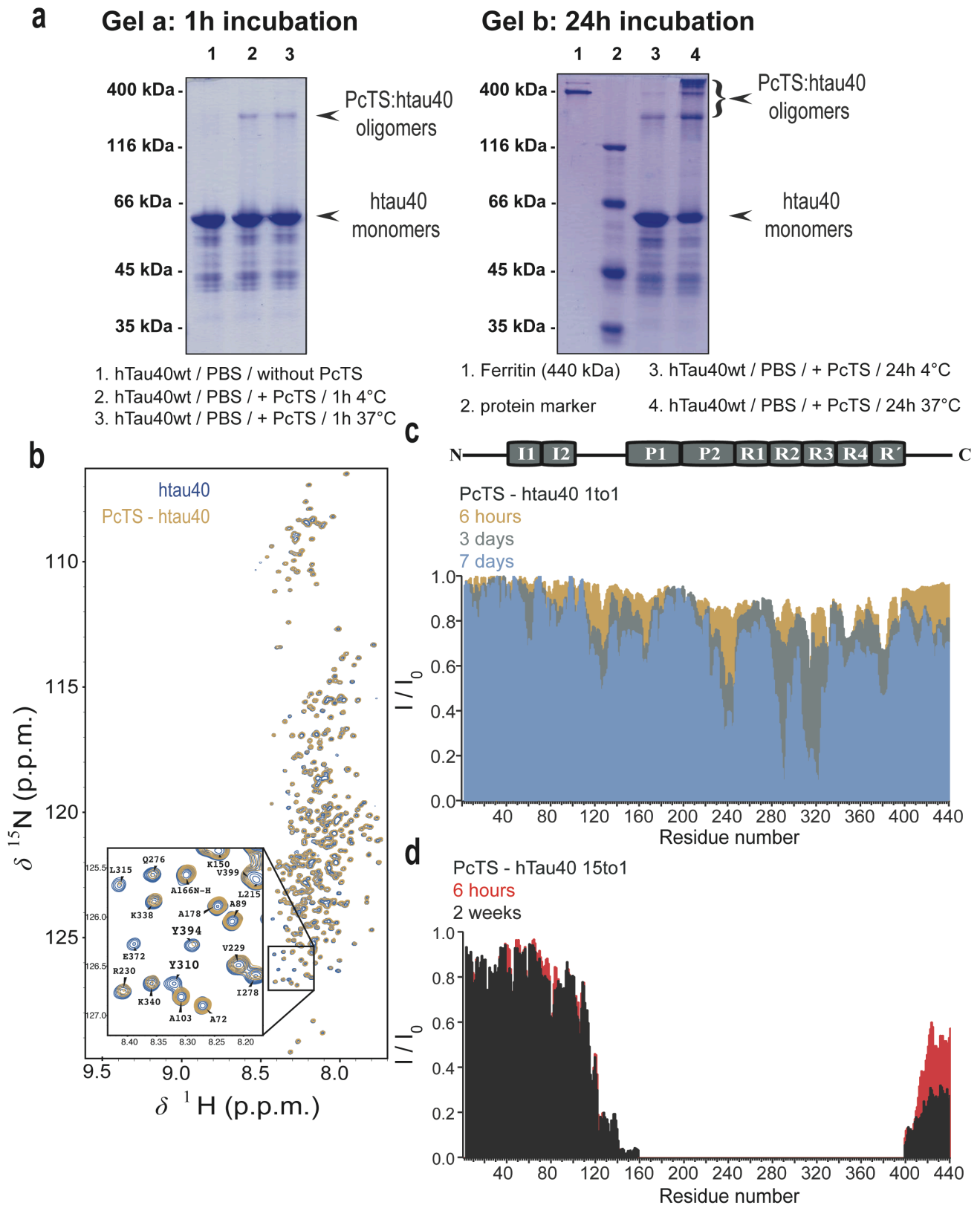


**Figure S3. Time-dependent remodeling of the PcTS-stimulated Tau oligomers.** (a) PcTS-induced oligomers visualized by SDS-PAGE. 50  $\mu$ M monomeric httau40 samples containing 1 mM DTT were prepared in PBS buffer (pH 7.4) and heated for 20 minutes at 95  $^{\circ}$ C. After incubation with 750  $\mu$ M PcTS for 1 or 24 hours at 4 or 37  $^{\circ}$ C, all samples were run on SDS-PAGE gels together with reference (Ferritin 440 kDa and protein marker) and control samples (monomeric httau40 in PBS buffers). The samples incubated for 1 hour at 4 and 37  $^{\circ}$ C show a protein band of higher molecular weight (gel a line 3 and 4). Further 23 hours of incubation, resulted in an intensity increase and the appearance of additional protein bands with a considerable decrease of the monomeric httau40 signal (comparison of gel a line 4 with gel b line 4). (b) Superposition of 2D  $^1$ H- $^{15}$ N HSQC spectra of 100  $\mu$ M httau40 in the absence (blue) and presence (yellow) of an equimolar ratio of PcTS. (c,d) Time-dependence of NMR signal intensity ratios of httau40 for (c) 1:1 PcTS-httau40 and (d) 15:1 PcTS-httau40.

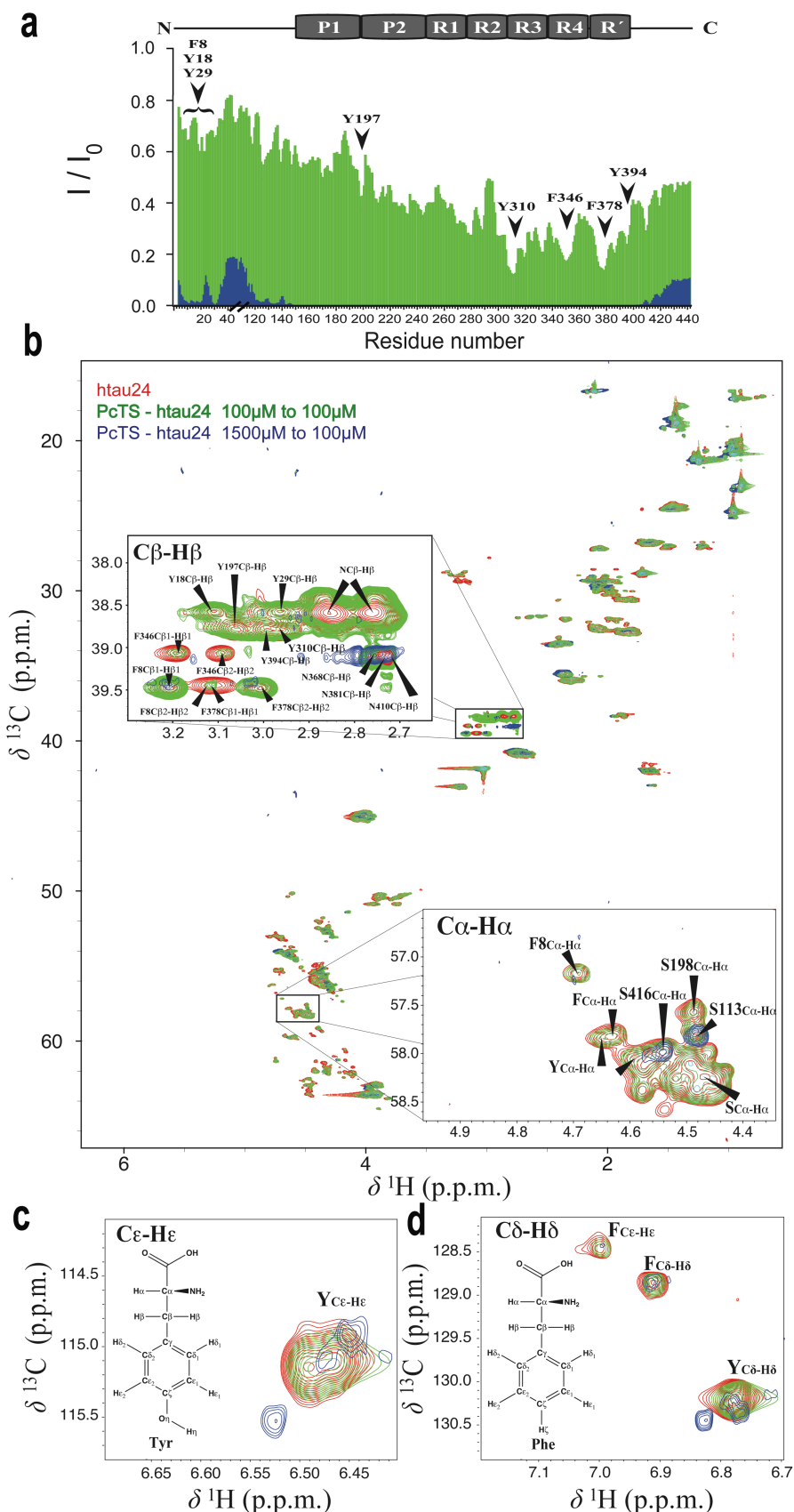


**Figure S4. Interaction of PcTS with the shorter Tau isoform htau24.** (a) Ratios of NMR signal intensities observed in 2D  $^1\text{H}$ - $^{15}\text{N}$  HSQC of 100  $\mu\text{M}$  htau24 (in 50 mM phosphate buffer pH 6.8) in the absence and presence of 100  $\mu\text{M}$  (green) and 1500  $\mu\text{M}$  (blue) PcTS. Residue numbers correspond to the sequence of htau40. The location of aromatic residues is indicated. Htau24 lacks the two negatively charged inserts (see domain organization on the top). (b) Overlay of the aliphatic regions from 2D  $^1\text{H}$ - $^{13}\text{C}$  HSQC spectra of htau24 in the absence (red) and presence of a 1-fold (green) and 15-fold (blue) excess of PcTS. The aliphatic and aromatic (c and d) regions of the spectra show a strong decrease in the NMR signal intensities of the aromatic residues upon compound addition and their disappearance at large excess of compound.

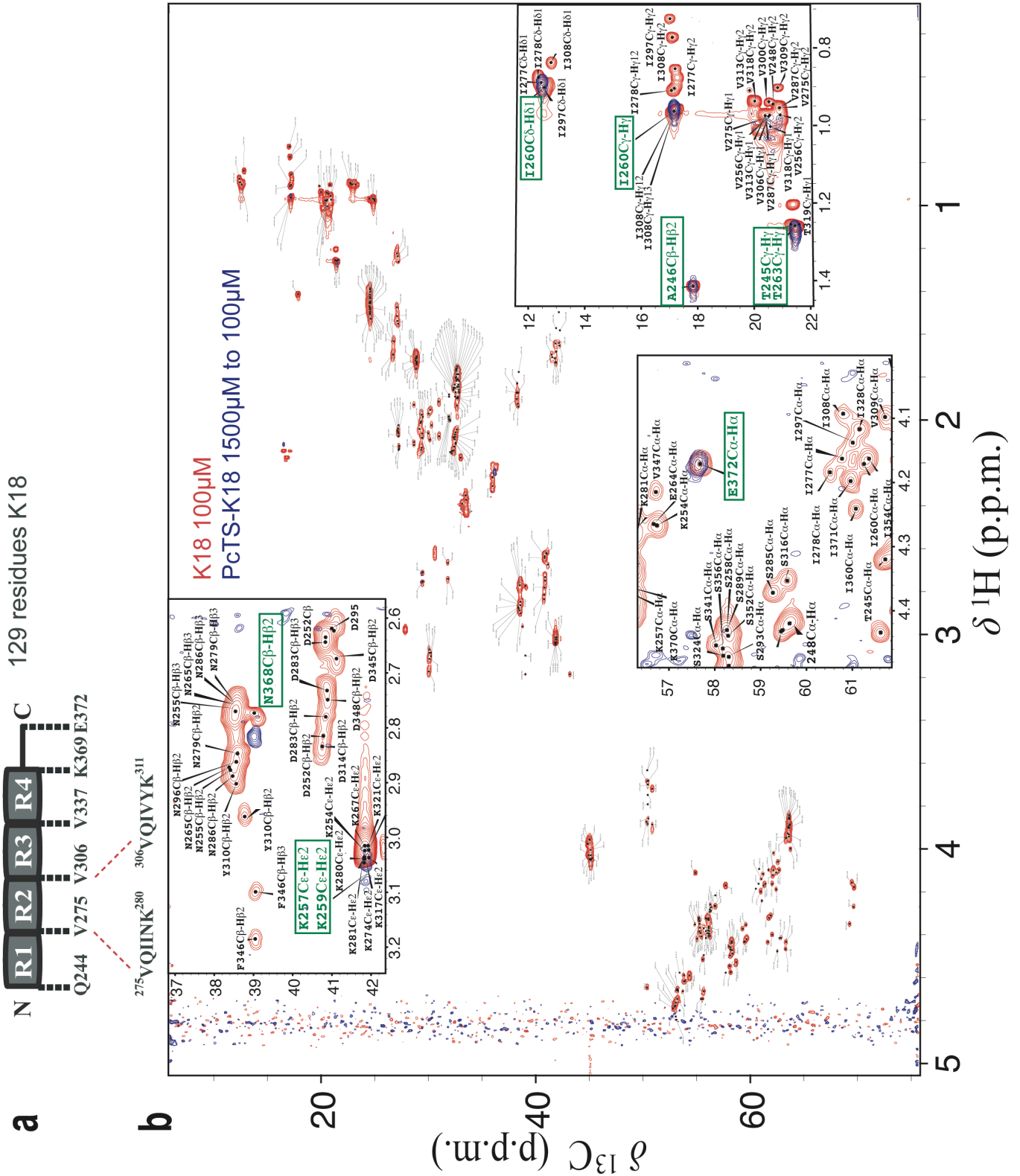


**Figure S5. Interaction of PcTS with the Tau fragment K18 that comprises only the repeat domain of htau40.** (a) Domain organization of K18. The two hexapeptides at the N-terminal ends of repeats R2 and R3 are highlighted. (b) Superposition of 2D  $^1\text{H}$ - $^{13}\text{C}$  HSQC spectra of 100  $\mu\text{M}$  K18 without (red) and with 15-fold (blue) excess of PcTS. The signals of all residues disappeared except for the highlighted resonances (green) that correspond to the flexible N- (A246, K257, K259, I260, and T263) and C- (N368 and E372) termini.

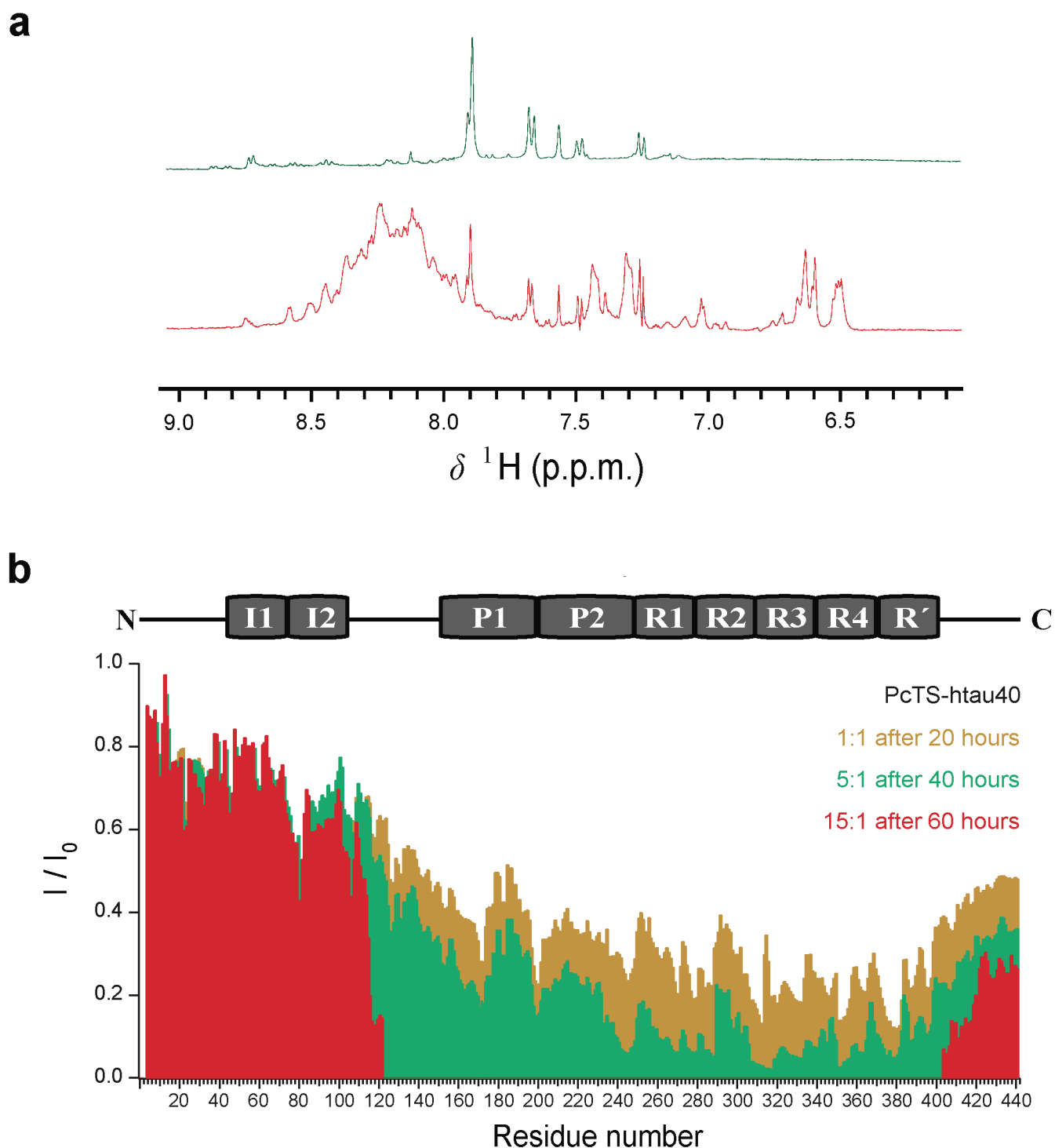


**Figure S6.** (a) 1D  $^1\text{H}$  NMR of PcTS alone (green) and in the presence of htau40 at a PcTS:htau40 molar ratio of 15:1 (red). The concentration of PcTS and the experimental parameters were identical in the two measurements. The reduction of the PcTS signal in the presence of htau40 suggests that about 40% of PcTS is incorporated into the Tau oligomers and therefore no longer visible in the 1D  $^1\text{H}$  NMR spectrum. (b) NMR broadening profiles observed at a 10-fold lower concentration of htau40 (10  $\mu\text{M}$ ) with the same PcTS:Tau molar ratio (1:1, yellow, 5:1 green, 15:1 red). The domain organization of htau40 is shown above.

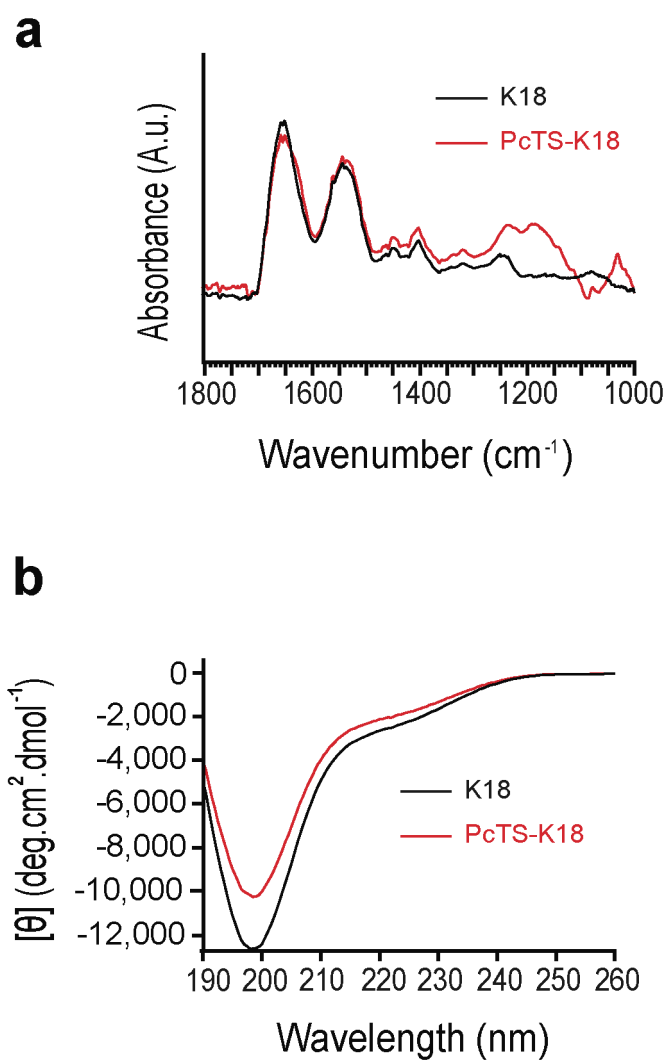


**Figure S7.** (a) FT-IR spectra of K18 in the absence (black) and presence of a 15-fold excess of PcTS (red). (b) Far UV-CD spectra of K18 in the absence (black) and presence of a 15-fold excess of PcTS (red).

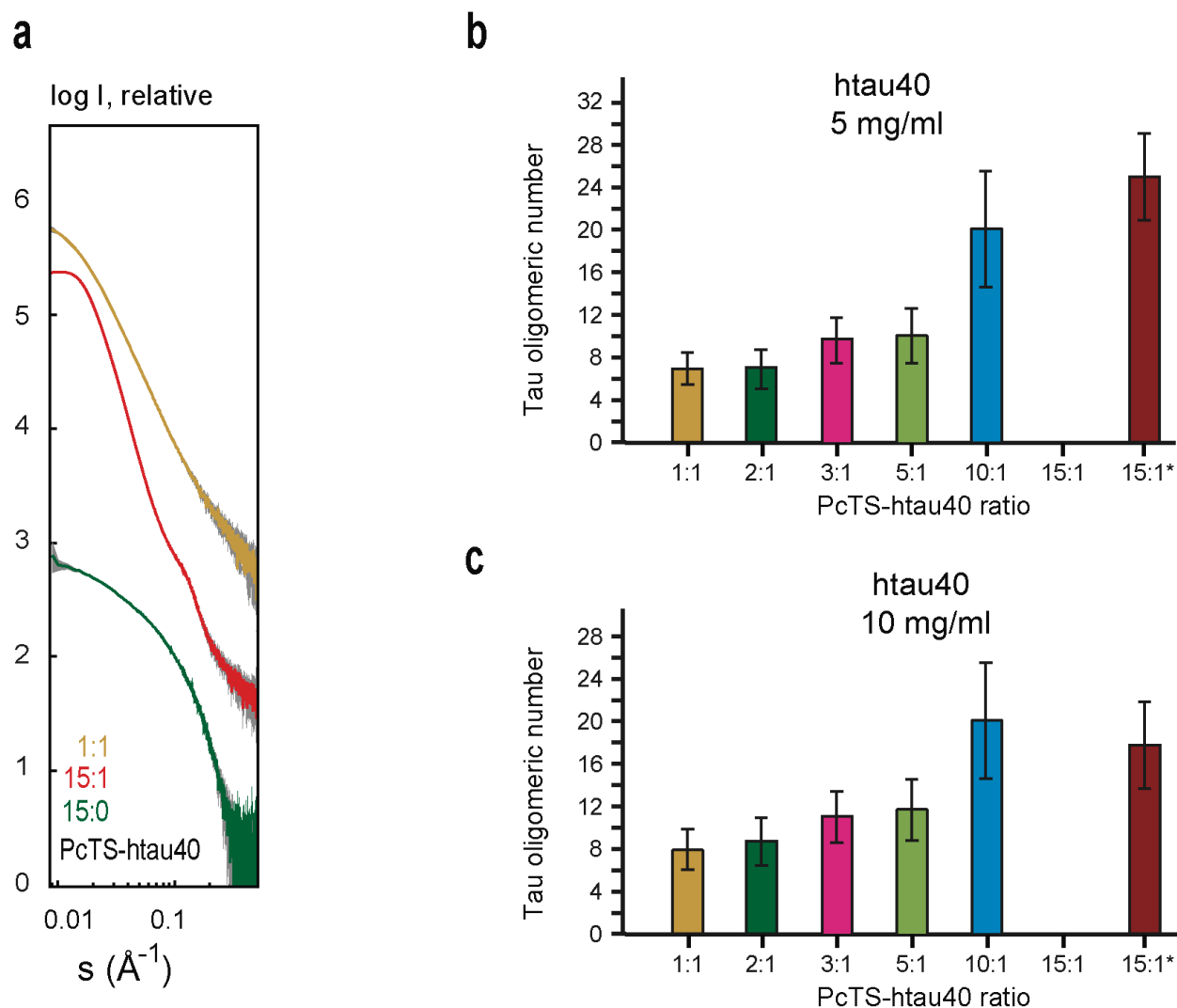


**Figure S8. SAXS of PcTS-stimulated Tau oligomers.** (a) SAXS profile of PcTS alone (green) and PcTS-htau40 profiles (1:1 orange and 15:1 red). The three profiles have been scaled based on the PcTS concentration, i.e. such that the PcTS concentration is effectively the same for the three profiles. Note that the scattering intensity for PcTS alone is much smaller and does not substantially contribute to the scattering of the Tau oligomers. (b,c) Estimation of the number of Tau molecules incorporated into the oligomers at different PcTS:htau40 ratios containing 5 (b) or 10 mg/ml (c) htau40. Samples with a PcTS:htau40 ratio of 15:1 were filtered (using a centrifugal filter with 0.2  $\mu\text{m}$  cutoff) prior to the SAXS measurements. Error bars were estimated from the standard error of  $I_0$  variations between different concentrations of htau40 but the same ratio of PcTS and accounting for the concentration of residual monomeric protein as determined by NMR (see Experimental Section for further information).



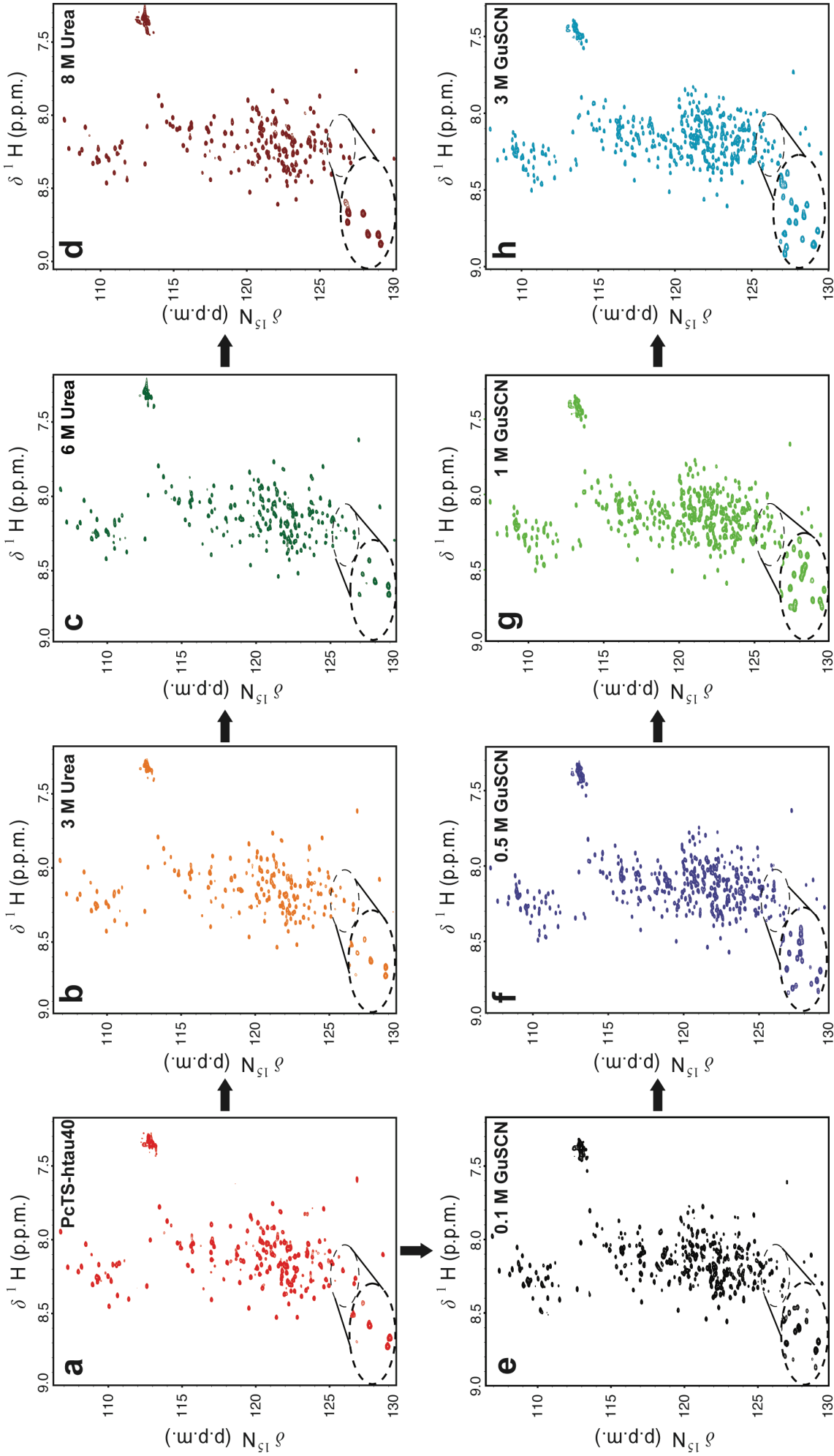


**Figure S9** - 2D  $^1\text{H}$ - $^{15}\text{N}$  HSQC spectra of PcTS-htau40 15to1 ratio (at pH 6.8 and  $5^\circ\text{C}$ ) in the (a) absence and presence of (b) 3 M, (c) 6 M, and (d) 8 M urea; or (e) 0.1 M, (f) 0.5 M, (g) 1 M and (h) 3 M GuSCN.

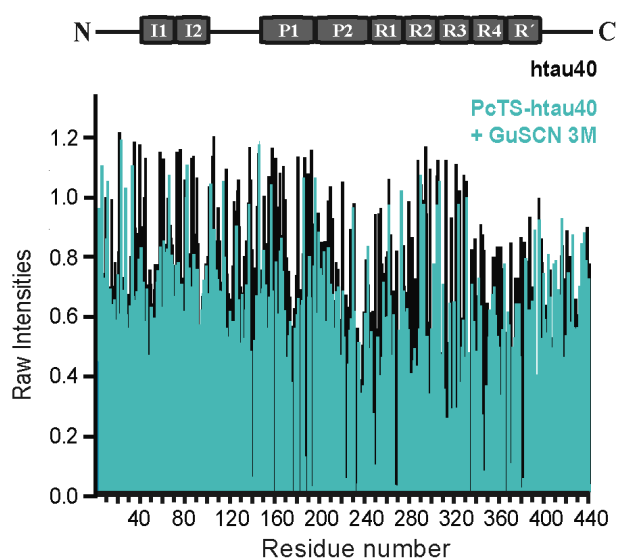


**Figure S10.** NMR signal intensities in 2D  $^1\text{H}$ - $^{15}\text{N}$  HSQC spectra of monomeric htau40 (black) and of htau40 in the presence of a 15-fold excess of PcTS and 3 M GuSCN (green). Intensities for all peaks are shown, both isolated and overlapped with other peaks and without 3-residue averaging. Signal intensities in the two spectra were normalized with respect to each other.